Indoor vs. outdoor aging – polymer degradation in PV modules investigated by Raman spectroscopy

C. Peike, T. Kaltenbach, K.A. Weiß, M. Koehl
Fraunhofer Institute for Solar Energy Systems (ISE), Heidenhofstr.2, D-79110 Freiburg, GERMANY

ABSTRACT

Indoor and outdoor aging tests are common methods for PV module degradation investigation. But to what extend are accelerated indoor aging tests comparable to outdoor exposure tests? The impact of indoor and outdoor tests on the polymer degradation in full-size PV modules was investigated. Polymer aging within a PV module is one of the major factors influencing module performance in the course of its lifetime. Degradation phenomena like yellowing, delamination or changes in the elastic modulus of the encapsulation may lead to transmission losses, corrosion effects or cell cracks. Raman Spectroscopy has recently been reported by our group as a non-destructive, analytical method for encapsulation degradation analysis. The degradation of the encapsulation of indoor and outdoor aged crystalline silicon PV modules was examined by the means of Raman Spectroscopy with special attention to the spatial-dependency of the degradation. The investigated modules were subjected to several different accelerated aging procedures with a systematic variation of the climatic conditions temperature, humidity and UV. Identical modules were aged in different climates (arid, tropical, urban and alpine) for up to three years. The degradation of the encapsulant was observed, resulting in an increasing fluorescence background in the Raman spectra. A dependency of the aging process on the relative position to the edges of the cell was found. The aging conditions appeared to influence the spatial distribution of the fluorescence and therefore, the polymer degradation, markedly. Furthermore, correlations between accelerated aging tests and outdoor exposure tests could be found.

Keywords: PV module, accelerated aging, outdoor aging, Raman Spectroscopy, encapsulation, Ethylene vinyl acetate, degradation.

1. INTRODUCTION

Indoor and outdoor aging tests are common methods for PV module degradation investigation. But to what extend are accelerated indoor aging tests comparable to outdoor exposure tests? Polymeric materials used in photovoltaic modules, which are mainly the encapsulation and the back-sheet, represent one of the most fragile parts of a module in terms of long term stability. In order to give longer life time guarantees and for enhancing the over-life performance of a module, the aging processes within a module have to be understood in depth. Raman Spectroscopy has recently been reported by our group as a tool for analyzing the encapsulation degradation, giving information about the extent of degradation before the module performance is decreasing [1]. The degradation of the encapsulation material of photovoltaic modules has been investigated over the past 20 years ([2], [3], [4], [5]), but hardly any attention has been paid to the spatial dependency of the aging process in a PV module. Depending on the relative position of the polymer to the cell, degradation can be accelerated or reversed. Inhomogeneities in the spatial distribution of the aging condition of the module components are induced by water vapor and oxygen diffusion processes [6], local heating due to hot spots [7], defect solder bonds or an inadequate edge isolation of the cell [8], [9]. The spatial distribution of the encapsulation degradation in c-Si PV modules was investigated by Raman Spectroscopy after different accelerated aging tests as well as after three years of outdoor exposure in different climates (moderate, tropic, mountain and arid). The comparison of the extent and distribution of the indoor and outdoor aging induced polymeric degradation is a basis for accelerated aging test enhancement.
In which way the fluorescence present in the Raman spectra of the aged modules is characteristic for a certain aging condition should be investigated. Special attention was paid to the shape of the fluorescence and distribution of the fluorescence intensity across the cell.

2. MATERIALS AND METHODS

2.1. Samples

The analyzed modules were full-size crystalline silicon PV modules of seven German manufacturers (S1 - S7). All modules had a similar design, consisting of solar-glass glazing, EVA encapsulation, polycrystalline or monocrystalline Si-cells, a Tedlar-PET-Tedlar (TPT) back-sheet and an aluminum frame. Exemplarily, the results of two module types will be presented in this paper. The performance values of the modules before aging and after the different accelerated and outdoor aging tests are given in tab.1. Heat, UV, UV/DH and all outdoor aging tests had only a minor impact on module performance (up to -2%) except for the mountain-aged module S7 which encountered severe cell breakage. In contrast to that, the damp-heat test caused severe performance losses of -73.4 or 61.6%, respectively.

Tab.1. Performance of the modules before and after the aging tests.

Aging test	S5			S7		
	P_0	P_1	ΔP	P_0	P_1	ΔP
	[W]		[%]	[W]		[%]
H	164.2	164.8	+0,4	211.9	207.6	-2.1
UV	157.0	156.9	-0,1	211.1	210.3	-0.4
UV/DH	164.0	161.7	-1,4	211.9	210.5	-0.6
DH	161.8	43.1	-73,4	211.8	81.3	-61.6
arid	158.8	157.1	-1.1	213.4	213.2	-0.1
tropic	158.9	158.8	-0.1	213.6	211.5	-1.0
moderate	160.9	160.1	-0.5	213.5	217.4	+1.7
mountain	158.5	160.5	+1.3	205.3	191.7	-6.3

2.2. Aging tests

One set of modules was exposed to a heat aging (H) at 90°C and ~0% r.h. in a climatic cabinet for 2000 h. Another set of modules was exposed to UV irradiation (UV) according to IEC6164 with a fluorescence tube (UV-B ≈15%) at 60°C, 0% r.h. and with a total dose of 240 kWh/m^2 for 1300 h. A further set of modules was exposed to UV radiation according to IEC61646 ed.2 (3-10% UV-B) in a climatic cabinet operating at 60% relative humidity and 60°C temperature (UV/DH). The sample temperatures varied between 80°C and 90°C depending on the module construction and its location in the cabinet. A total UV-dose of 108 kWh/m² was obtained after 950 h exposure. The UV-light source is described elsewhere [10]. The so called damp-heat ageing test (DH) was conducted according to IEC61215 (85% r.h. at 85°C) for up to 4000 h. An overview of the aging tests and conditions is given in tab.2.

Tab.2. Accelerated aging test conditions.

Aging test	Abbreviation	Aging conditions
No aging	ref	-
Heat aging	H	90°C/~0% r.h., 2000 h
UV aging	UV	60°C, 0% r.h., 240 kWh/m^2,1300 h
UV/ damp heat aging	UV/DH	60°C, 60% r.h., 108 kWh/m^2, 950 h
Damp heat	DH	85°C, 85% r.h., 4000h

The exact conditions of the outdoor exposition of the modules is described by Koehl et al [11]. The measured average ambient temperature and relative humidity, as well as the maximum and minimum temperature and the average annual sum of global irradiance G are given in tab.3. The distribution of the average measured module temperature at the four different test sides shows a broad distribution in the arid, mountain and moderate climate and a very sharp distribution with a maximum at 23°C in the tropic climate (fig.1). At all test sites and especially in the arid and tropic climate, a shoulder up to 65°C due to the heating of the modules during day-time can be found.

Tab.3. Climatic conditions during the outdoor aging tests.

Aging test	climate	T_{AV}	T_{MAX}	T_{MIN}	$R.H._{AV}$	G
		[°C]			[%]	[kWh/am^2]
Negev, Israel	arid	18	39	-5	69	2269
Serpong, Indonesia	tropic	27	21	19	79	1626
Cologne, Germany	moderate	12	36	-14	76	1184
Zugspitze, Germany	mountain	0	21	-25	78	1169

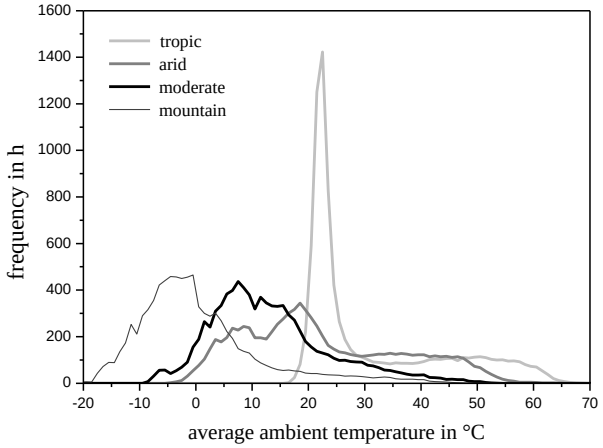

Figure 1. Frequency distribution of the average measured module temperature at the four different test sides [12].

2.3. Methods

Raman Spectroscopic measurements were carried out using a WiTec Alpha 500 Raman Microscope with a remote Raman probe. A detailed description of the measurement set up can be found in literature [1]. Analogous cells in the middle of each module were measured horizontal across the cell. Furthermore, extraordinary cells like cells with a crack or an inactive region showing up in the electroluminescence image were measured. All spectra were normalized on 90 cm^{-1} in order to maintain the information of relative fluorescence intensities as measured.

3. RESULTS AND DISCUSSION

3.1. Raman spectra

The Raman spectra of module types S5 and S7 before and after accelerated aging and outdoor aging are shown in fig.2 and fig.3, respectively. The reference spectra show the major EVA vibrations at 629 (v(OCO)), 1068 (v(CC)), 1126 (v(CC)), 1295 (t(CH)), 1438 (d(CH)), 1724 (v(CO)), 2832, 2863, 2880, 2895 and 2913cm^{-1} (v(CH_2) and v(CH_3)).
In the Raman spectra of all aged modules, fluorescence was present. As a first step, a qualitative overview of the shape of the fluorescence and its distribution across the cell should be given.
For module type S5, the heat aging caused little fluorescence and the EVA Raman vibrations remained very intense across the whole cell. After damp-heat aging, the fluorescence of module S5 was high at the edges of the cell and low in the middle. Only traces of the EVA vibrations were visible at the edges. UV aging resulted in a very intense fluorescence with a strong fine structure. At the very edges of the cell, the fluorescence was much lower than in the middle and EVA vibrations were detectable. UV / damp-heat aging induced Raman spectra similar to those after UV aging, with the difference of a slightly higher fluorescence at the edges of the cell. Of the outdoor exposition sites, the moderate and especially the mountain site caused least fluorescence. After aging at the mountain site, no EVA vibrations were detectable in the middle of the cell, spectra at the edges were similar to the reference spectra. In contrast to that, the module aged at the moderate exposition site showed slightly weakened EVA vibrations in the middle of the cell and also very good EVA spectra at the edges. The tropic as well as the arid climate induced a very strong fluorescence. The module aged in the tropics showed Raman spectra similar to that after UV aging with regard to the fluorescence intensity, fine structure and fluorescence intensity distribution but exhibited a broader region of low fluorescence and good EVA spectra about 3 cm from each edge. The arid exposition site also caused a very intense fluorescence with a less intense fine structure than UV aging or the tropic exposition site.

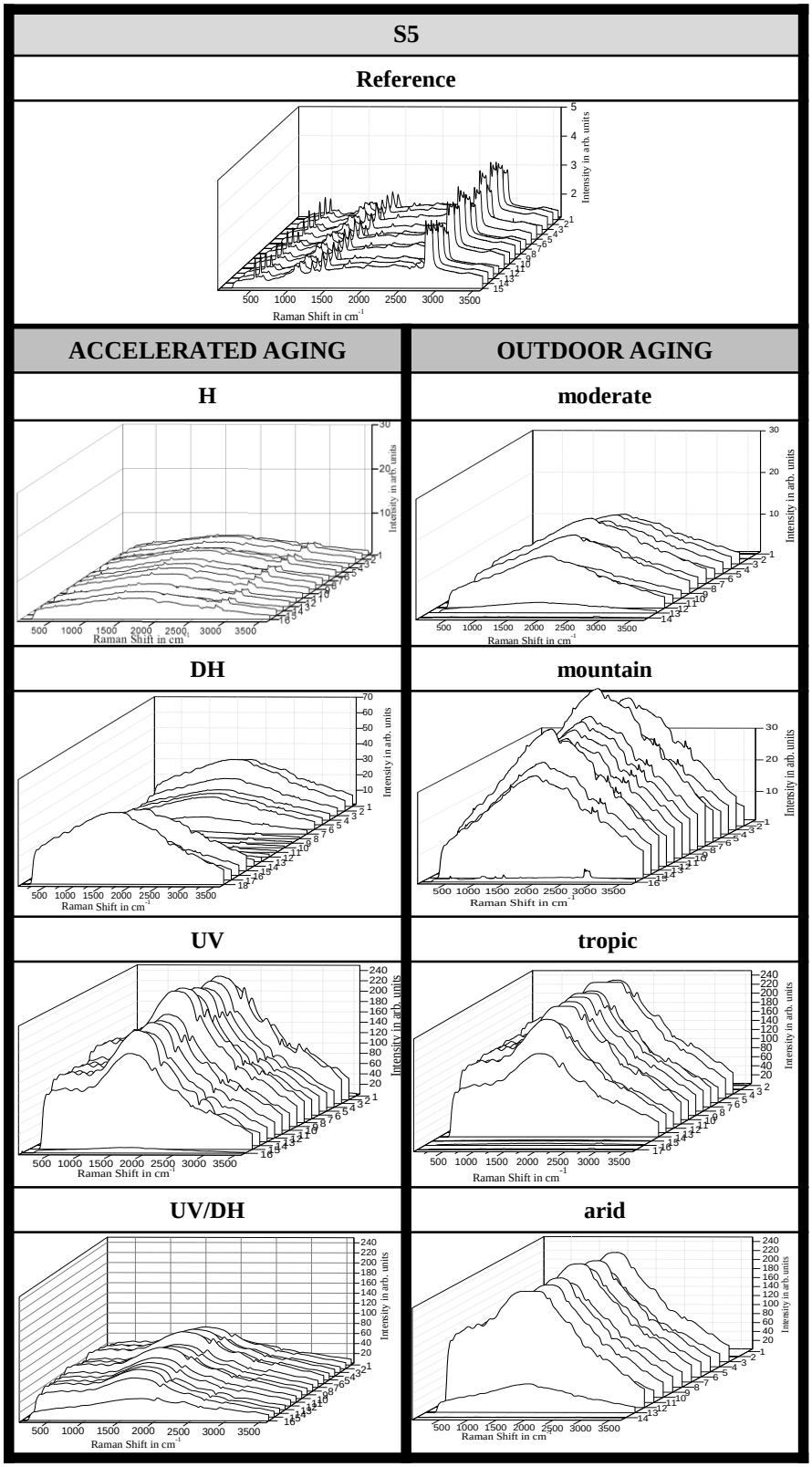

Figure 2. Raman spectra across one cell in modules type S5 after the different accelerated aging tests and three years of outdoor exposure.

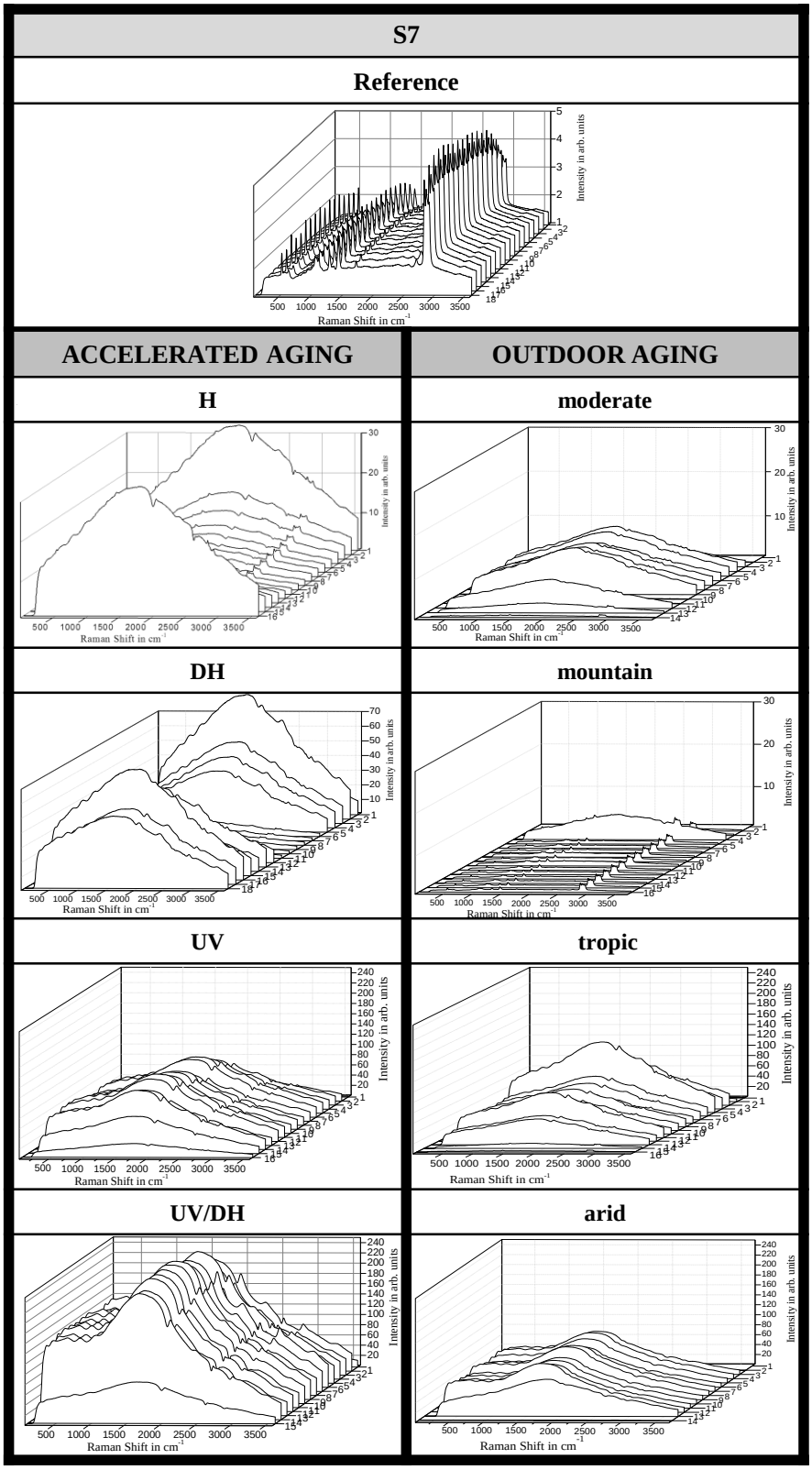

Figure 3. Raman spectra across one cell in modules type S7 after the different accelerated aging tests and three years of outdoor exposure. The cells in modules S7-moderate and S7-mountain were cracked (see Fig.5c and d).

Module type S7 showed, compared to module S5-H, a very different distribution of Raman spectra across the cell after heat aging with high fluorescence at the very edges of the cell and good EVA spectra in the cell center. The Raman spectra of S7 after damp-heat aging were completely overshadowed by fluorescence in the region of the outer 5 cm of the cell. No fluorescence was visible in the center of the cell. The UV and UV/DH aged modules of type S7 showed slightly similar results: fluorescence was high (UV) or very high (UV/DH) in the middle and lower at the edges, a fine structure could be found being more intense after UV/DH aging.
The cell investigated in the S7 modules outdoor aged in moderate and mountain climate exhibited cracks near the solder bond (S7-moderate) and at several points across the whole cell (S7-mountain)(fig. 5 c and d). The mountain-aged S7 module showed extremely good EVA spectra, comparable to the reference spectra, across the whole cell. This effect is most likely due to the large number of cracks enabling oxygen to permeate through the cell intersections and induce photo-bleaching. The S7 module after aging in moderate conditions exhibited low fluorescence with no fine structure. Exposition in an arid environment led to intense fluorescence in the center of the cell and good EVA spectra at the outer two cm of the cell. Traces of the EVA vibrations were also detectable in the middle of the cell. The aging in an arid climate caused no fine structure and no EVA vibrations could be detected.
In terms of fluorescence intensity, fine structure and intensity distribution, the modules S5 and S7 aged under the most demanding climatic conditions of the arid and tropical environment appeared to be most similar to the UV-aged modules.

3.2. Influence of aging conditions on fluorescence intensity distribution

Fig. 4 and 5 show the distribution of fluorescence intensities at several equidistant points across one cell before aging, after accelerated aging (a) and outdoor exposition (b). For both module types, fluorescence intensities were very low and homogeneously distributed across the cell before aging (about two arb. units). After heat aging, module S5 showed a slight fluorescence of about 5 arb. units which was homogeneously distributed across the cell (fig. 4a). In contrast to that, the fluorescence intensity distribution of module S7-H exhibited a parabolic behavior with values varying between 30 arb. units at the edges and 7 arb. units in the middle of the cell. The fluorescence intensities of S7-H were comparable to the S7-DH module which showed a more linear decrease in fluorescence intensity towards the middle of the cell. For the DH-aged module S5, a plateau of low fluorescence (10 arb. units) in the cell center and a region of high fluorescence (around 50 arb. units) at the outer parts of the cell were found. Fluorescence increased slightly towards the edges and decreased about 30% at the very edge of the cell. The UV as well as the UV/DH aged modules exhibited a fluorescence distribution of very high and homogeneously distributed fluorescence in the center of the cell (S5-UV: 240, S7-UV: 110, S5-UV/DH: 90, S7-UV/DH: 250 arb. units) and an abrupt decrease in fluorescence intensity at the edges (S5-UV: -92%; S7-UV: -83%, S5-UV/DH: -45%, S7-UV/DH: -70%).
Outdoor aging caused a very similar fluorescence intensity distribution for all modules: fluorescence intensity was high in the middle of the cell and decreased abruptly at the edges of the cell (-95 to -99%). The intensity in the middle of the cell was equally high after aging in the arid and tropic climate for both module types, respectively. Both modules aged in the tropical climate showed a slightly higher fluorescence at the edges of the cell than the modules aged in an arid environment. For module type S5, the moderate and mountain exposition site resulted in a less intense fluorescence in the center of the cell (S5-moderate: 12 , S5-mountain: 40 arb. units) and in a slightly less abrupt decrease in fluorescence intensities at the edges (S5-moderate: -88%, S5-mountain: -95%). Due to the cracked cells in modules S7-mountain and S7-moderate, it can only be estimated that the moderate climate induced a similar fluorescence distribution in module S7 as in module S5 based on the observation of the non-cracked left part of the cell.

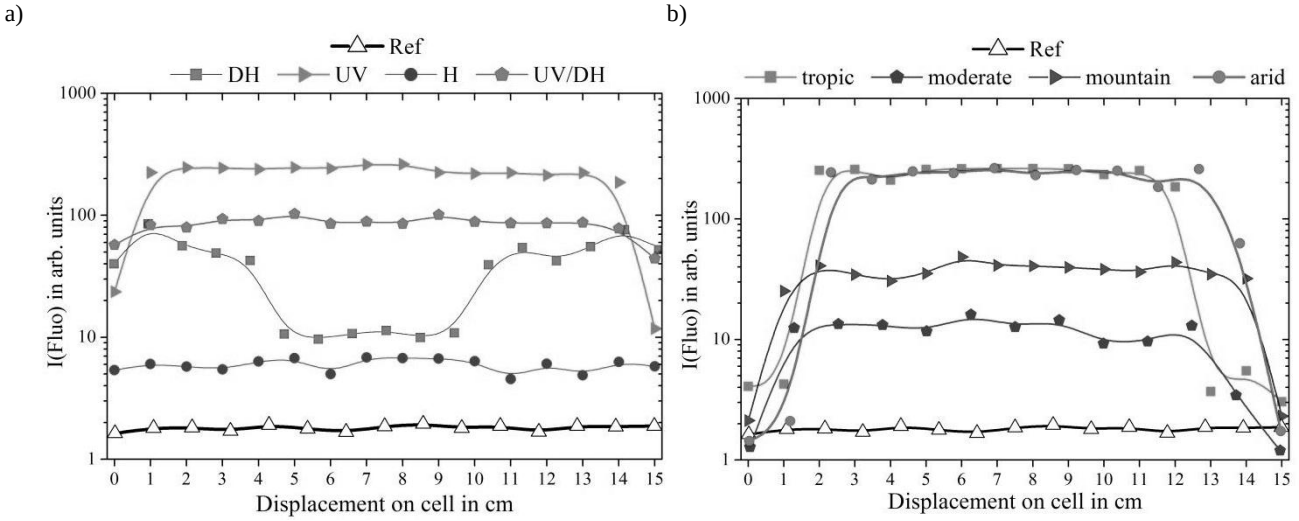

Figure 4. Fluorescence intensity distributions from Raman spectra measured across one cell of modules type S5 after the different accelerated aging tests (a) and outdoor exposure for three years, respectively (b).

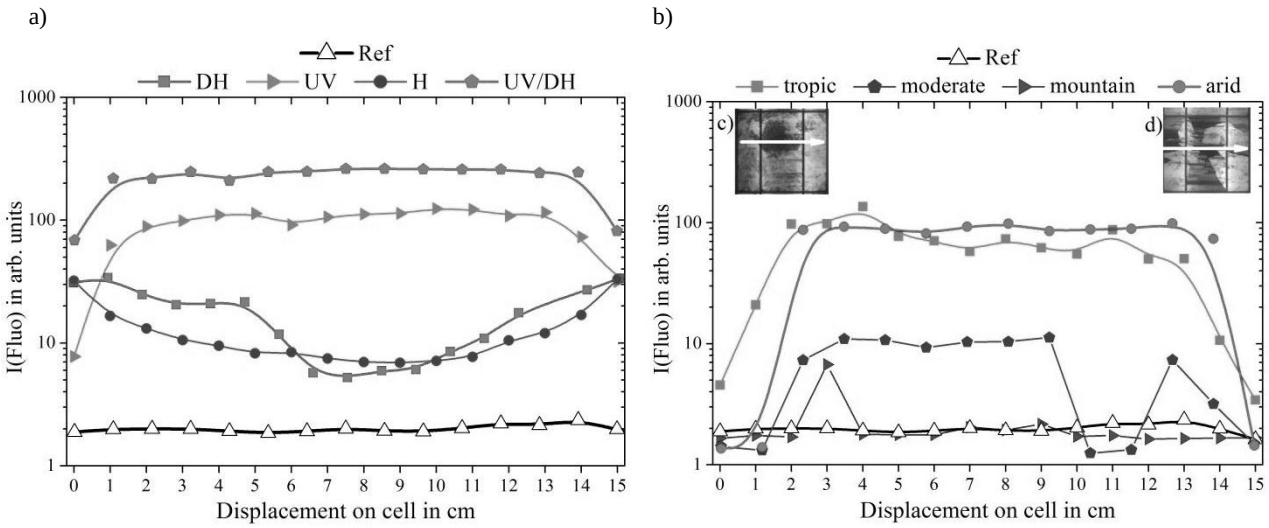

Figure 5. Fluorescence intensity distributions from Raman spectra measured across one cell of modules type S7 after the different accelerated aging tests (a) and outdoor exposure for three years (b), respectively. The cells in modules S7-moderate and S7-mountain were cracked as can be seen in the electroluminescence pictures (moderate - c and mountain -d).

4. CONCLUSION

The influence of the aging conditions on the spatial distribution of polymeric aging acoss a cell, manifested in a fluorescence background in the Raman spectra, was investigated.

Heat aging either caused a homogeneous aging across the cell or an increasing fluorescence towards the edges, depending on the specific materials used in the module. Damp-heat aging turned out to induce a higher fluorescence at the edges than in the center of the cell which can be explained by the only possible permeation pathway for water vapour permeating through the back-sheet into the back-side EVA and finally towards the front-side EVA where it causes degradation reactions like hydrolysis.

The presence of UV during aging resulted in a fluorescence distribution across the cell which is absolutely not comparable to that induced by damp-heat or heat aging. Especially the UV aging with 240 kWh/m^2 caused a fluorescence similar to that after outdoor exposition in an arid and tropical climate for three years, both in terms of fluorescence distribution, intensity and fine structure. The EVA in front of cracked cells showed an altered aging behavior, most likely due to photo-bleaching reactions which are also responsible for an abrupt decrease in fluorescence intensity at the edges of all cells in UV, UV/DH or outdoor aged modules.
A subject of our current research is the investigation of the origin of the fluorescence as well as the examination of the nature of the fine structure of the fluorescence.

ACKNOLEDGEMENT

The work was partly funded by the German Federal Ministry for the Environment, Nature Conservation and Nuclear Safety (BMU FKz 0329978) and sponsored by the industrial partners Scheuten Solar, Schott Solar, Solar Fabrik, Solarwatt, SolarWorld and Solon.

REFERENCES

1. Peike, C., et al., *Non-destructive degradation analysis of encapsulants in PV modules by Raman Spectroscopy.* Solar Energy Materials and Solar Cells **95**(7), 1686-1693 (2011).
2. Glick, S.H., et al. *Performance degradation of encapsulated monocrystalline-Si solar cells upon accelerated weathering exposures. Proc. 2001 NCPV Program Review Meeting* (2001).
3. Pern, F.J., et al. *Weathering degradation of EVA encapsulant and the effect of its yellowing on solar cell efficiency*. Proc. *22nd IEEE Photovoltaic Specialists Conference* (1991).
4. Pern, F.J., *Ethylene-vinyl acetate (EVA) encapsulants for photovoltaic modules: Degradation and discoloration mechanisms and formulation modifications for improved photostability.* Die Angewandte Makromolekulare Chemie **252,** 195-216 (1997).
5. Allen, N.S., et al., *Aspects of the thermal oxidation, yellowing and stabilisation of ethylene vinyl acetate copolymer.* Polymer Degradation and Stability **71**(1), 1-14 (2000).
6. Huelsmann, J.P., et al. *Numerische Simulation der Feuchtebelastung von PV-Modulen für unterschiedliche Klimastandorte*. Proc. *41. Jahrestagung der GUS* (2012).
7. Alonso-García, M., J. Ruiz, and F. Chenlo, *Experimental study of mismatch and shading effects in the I-V characteristic of a photovoltaic module.* Solar Energy Materials and Solar Cells **90**(3), 329-340 (2006).
8. Quintana, M.A., et al. *Commonly observed degradation in field-aged photovoltaic modules*. Proc. *29th IEEE Photovoltaic Specialists Conference* (2002).
9. Dechthummarong, C., et al., *Physical deterioration of encapsulation and electrical insulation properties of PV modules after long-term operation in Thailand.* Solar Energy Materials and Solar Cells **94**(9), 1437-1440 (2010).
10. Koehl, M., et al. *Development and application of a UV light source for PV-module testing*. *Proc. 24th European Photovoltaic Solar Energy Conference* (2009).
11. Koehl, M. and M. Heck. *Load evaluation of PV-modules for outdoor weathering under extreme climatic conditions*. Proc. *4th European Weathering Symposium* (2009).
12. Koehl, M., et al., *Modeling of the nominal operating cell temperature based on outdoor weathering.* Solar Energy Materials and Solar Cells **95**(7),1638-1646 (2011).